Supporting information

Th@C_1(11)-C_{86} : Actinide Encapsulated in an Unexpected C_{86} Fullerene Cage

Yaofeng Wang, [a†] Roser Morales-Martínez ,[b†] Wenting Cai,[c†] Jiaxin Zhuang,[a] Wei Yang [a] Luis Echegoyen,[c] Josep M. Poblet,[b] Antonio Rodríguez-Fortea,*[b] and Ning Chen*[a]

[a] *Laboratory of Advanced Optoelectronic Materials, College of Chemistry, Chemical Engineering and Materials Science, Soochow University, Suzhou, Jiangsu, 215123 (P. R. China)*

[b] *Departament de Química Física i Inorgànica, Universitat Rovira i Virgili, c/Marcel·lí Domingo 1, 43007 Tarragona (Spain)*

[c] *Department of Chemistry, University of Texas at El Paso, 500 W University Avenue, El Paso, Texas 79968 (United States)*

Table of Contents

High-performance liquid chromatography (HPLC) separation process of Th@C_1(11)-C_{86}. The first stage was performed on a BPM column (25 mm × 250 mm, Cosmosil Nacalai Tesque) with toluene as mobile phase. After that, as shown in Figure S1, fraction from 61 to 67 min (marked in blue) was re-injected into a BPD column (10 mm × 250 mm, Cosmosil Nacalai Tesque) for the second stage separation using toluene as the eluent. The fraction marked in green, which contained Th@C_{86} was collected. The third stage of separation was conducted on a BP column (10 mm × 250 mm, Cosmosil Nacalai Tesque) using toluene as the eluent, and pure Th@C_{86} was finally obtained. The purity of the isolated Th@C_{86} was then reconfirmed by chromatography on a Buckyprep column (10 mm × 250mm, Cosmosil Nacalai Tesque) with toluene at a flow rate of 4.0 mL/min, along with the MALDI-TOF mass spectrometry in a positively charged mode (Figure 1).

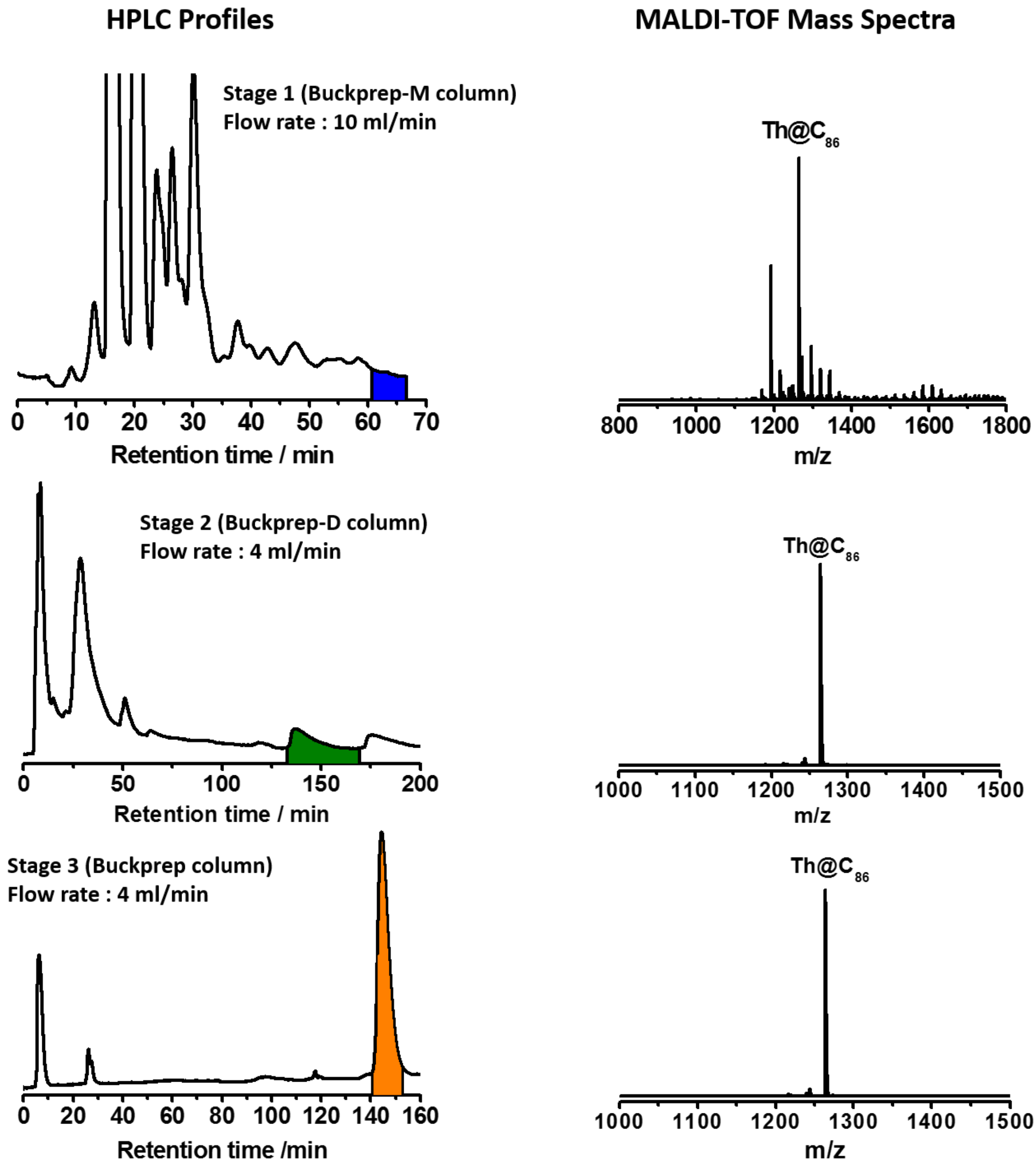

Figure S1. HPLC profiles showing the separation procedures of Th@C_{86} (left) and the corresponding MALDI-TOF mass spectra (right).

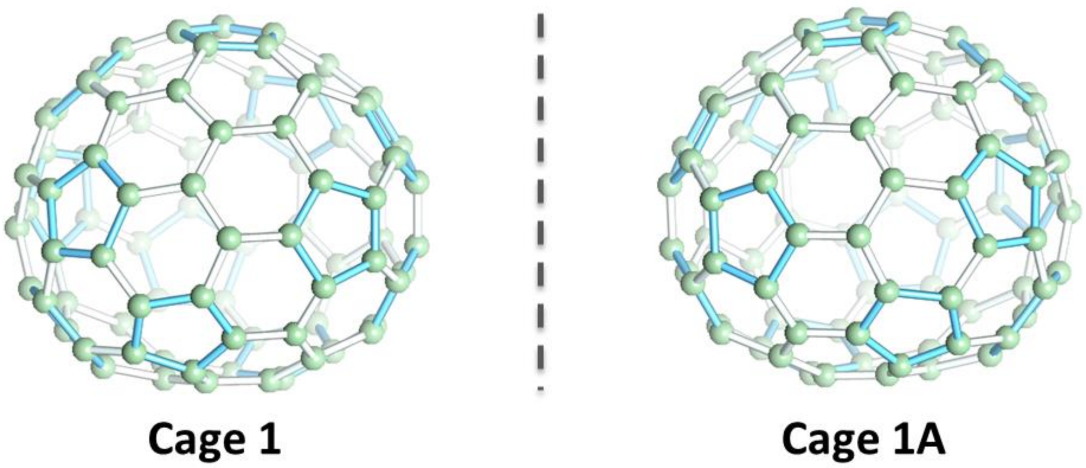

Figure S2. Structures of two enantiomers of Th@C_1(11)-C_{86}. Internal disordered sites of thorium atoms omitted for clarity.

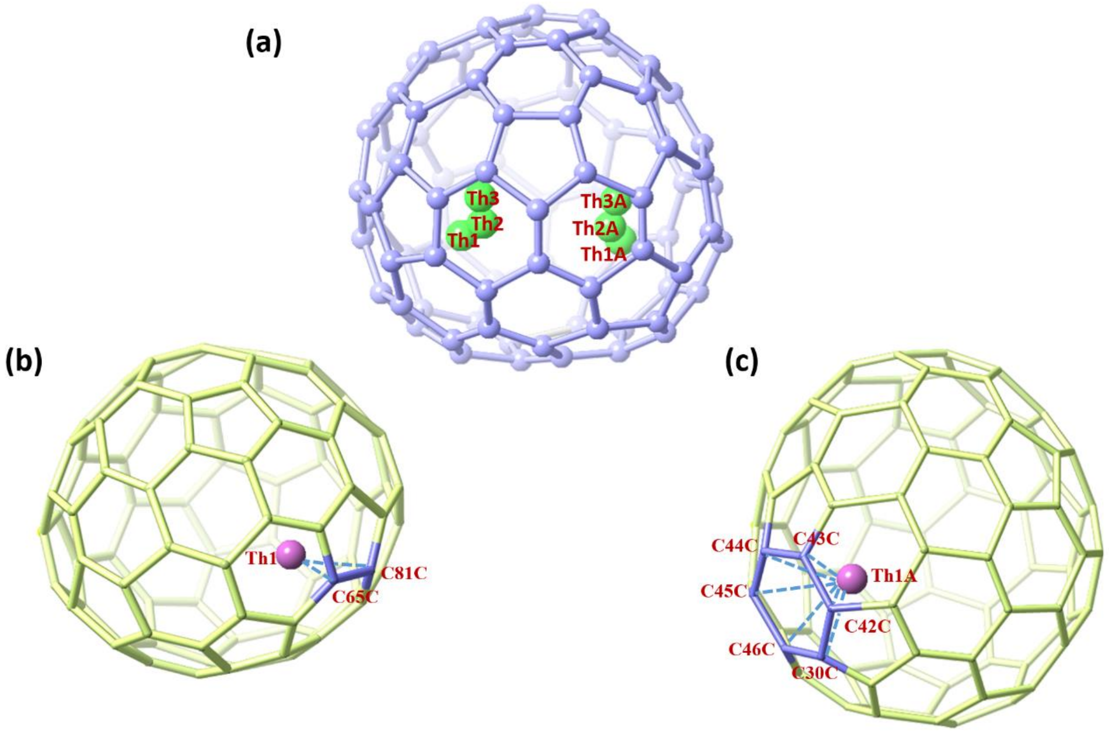

Figure S3. (a) Perspective drawing shows three positions (Th1, Th2 and Th3) and the mirror-related site (Th1A, Th2A and Th3A) of the disordered thorium sites in Th@C_1(11)-C_{86}. (b) The interaction of the major Th site Th1 with the closest cage portion. (c) The interaction of Th1A (the mirror-related site of Th1) with the closest cage portion.

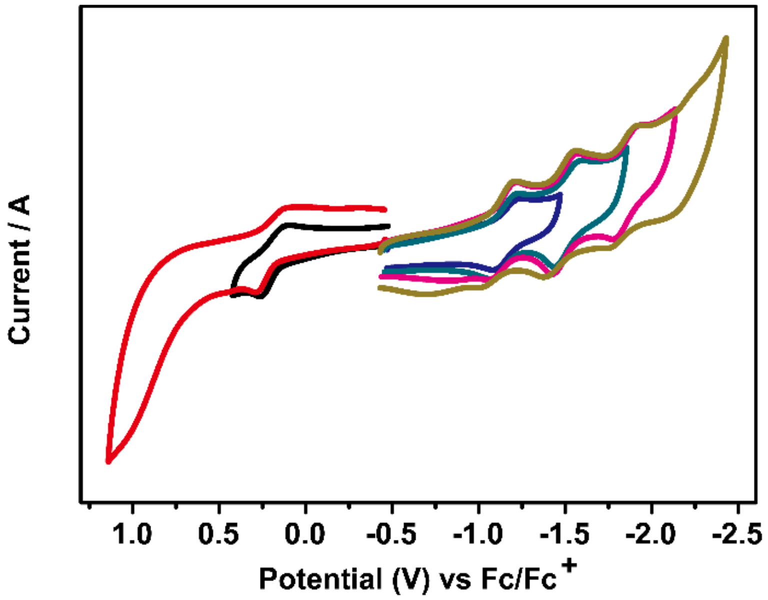

Figure S4. Cyclic voltammogram of Th@C_1(11)-C_{86}. Solvent: *o*-dichlorobenzene (with 0.05 M (*n*-Bu)4NPF6). Scan rate 100 mV/s.

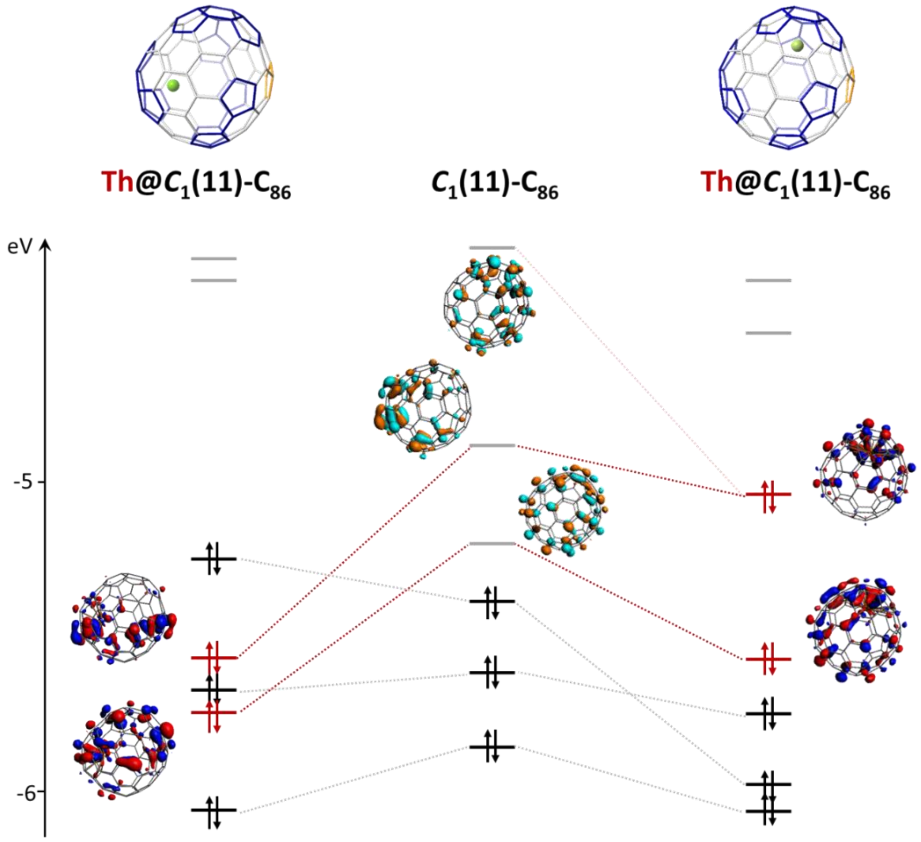

Figure S5. Simplified molecular orbital diagram interaction between the empty cage and the Th@C_1(11)-C_{86} with the most stable Th site (left) and the second one (right). Red arrows are used to represent the four electrons transferred from the Th to the lowest unoccupied orbitals of the fullerene cage. Dotted lines show the major orbital interaction contribution, in red the corresponding orbitals involving the electron transfer. Pyracylene (and sumanene) pentagon units are coloured in blue, the remaining pentagon in orange, and the Th is coloured in lime green.

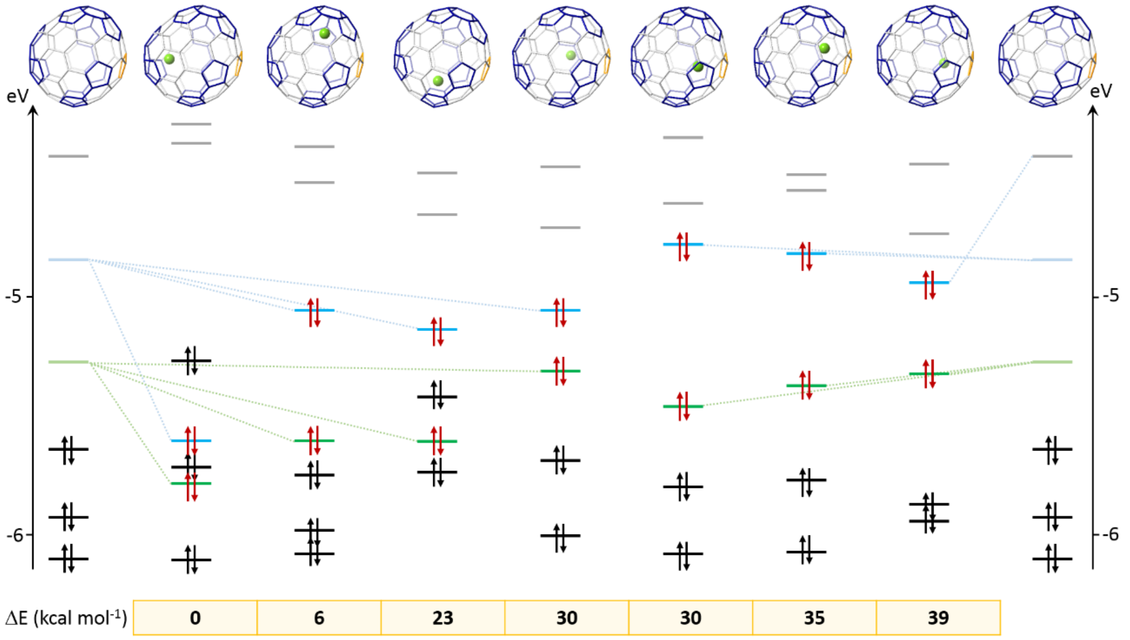

Figure S6. Simplified molecular orbital diagram between the empty cage (left and right) and the Th@C_1(11)-C_{86} for all the computed Th sites (relative energies in kcal·mol^{-1} at the bottom). Red arrows are used to represent the four electrons transferred from the Th to the lowest unoccupied orbitals of the fullerene cage. Dotted lines show the major orbital interaction contribution, in green for the corresponding LUMO of the empty cage and in blue for the LUMO+1.

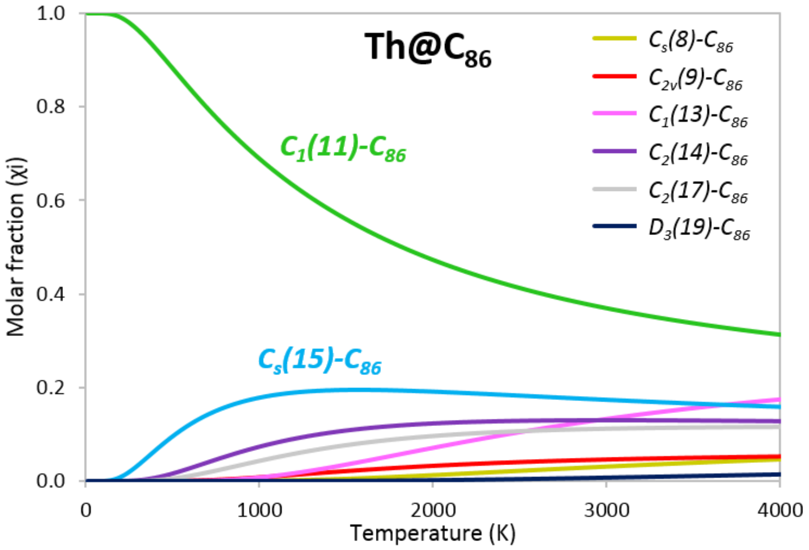

Figure S7. Computed molar fraction as a function of the temperature (K) using the free-encapsulating model (FEM) for the optimised isomers of Th@C_{86}.

Table S1. Occupancies of disordered thorium sites in Th@C_1(11)-C_{86}.

Labelling	**Th1**	**Th2**	**Th3**
Occupancy	0.310(3)	0.174(3)	0.016(2)

Table S2. Closest Th-Cage contacts in Th@C_1(11)-C_{86}.

Labelling	**Th1-C65C**	**Th1-C81C**	**Th1A-C30C**	**Th1A-C42C**	**Th1A-C43C**	**Th1A-C44C**	**Th1A-C45C**	**Th1A-C46C**
Length/Å	1.921	2.008	2.457	2.410	2.387	2.379	2.390	2.326

Table S3. Relative energies in kcal·mol^{-1} for neutral and tetraanionic C_{86} and endohedral Th@C_{86} for the selected IPR isomers.

isomer[a]	**#IPR**	**Sym**	**C_{86}**	**C_{86}^{4-}**	**Th@C_{86}**
8	8	C_s	26.4	9.1	13.8
9	9	C_{2v}	31.4	0.0	7.3
11	11	C_1	8.0	18.7	0.0
13	13	C_1	11.5	12.5	10.6
14	14	C_2	17.0	14.5	3.3
15	15	C_s	16.6	9.0	1.9
17	17	C_2	0.0	22.3	4.7
19	19	D_3	17.3	14.1	20.1

We have recently reported the motion of U@C_{80} at 300 and 1500 K [1] using Car-Parrinello molecular dynamics (CPMD) simulations. Although at room temperature the ion has limited mobility, at the temperature of fullerene formation it presents much more mobility inside the fullerene. For this reason the FEM model proposed by Slanina is used.[2, 3] Chirality contribution is also taken into account.[4]

Experimental details

Synthesis and Isolation of Th@C_{86}. The carbon soot containing thorium metallofullerenes was synthesized in a modified direct-current arc discharge Krätschmer-Huffman reactor with a mixture of ThO_2/graphite powder (molar ratio of M/C=1:24) under 200 Torr helium atmosphere. The resulting soot was refluxed in chlorobenzene in an argon atmesphere for 12 h. Multistage HPLC separations gave pure isomer Th@C_{86}, using columns including Buckyprep M column(25×250 mm, Cosmosil, Nacalai Tesque Inc.), Buckprep-D column(10×250mm, Cosmosil, Nacalai Tesque,Japan),and Buckprep column(10×250mm, Cosmosil, Nacalai Tesque, Japan). **Single-crystal X-ray diffraction.** Crystalline blocks of Th@C_{86}·[Ni^{II}(OEP)] were obtained by layering a benzene solution of Ni^{II}(OEP) over a nearly saturated solution of the endohedral in CS_2 in a glass tube. XRD measurements were performed at 120 K using a diffractometer (APEX II; Bruker Analytik GmbH) equipped with a CCD collector. The multi-scan method was used for absorption correction. The structure was resolved using a direct method and refined with SHELXL2013 [5]. Hydrogen atoms were inserted at calculated positions and constrained with isotropic thermal parameters.

Crystal data for Th@C_1(11)-C_{86}·[Ni^{II}(OEP)]·CS_2·C_6H_6 : $C_{129}ThNiN_4S_2H_{50}$, Mw = 2010.58, monoclinic, space group C2/m, a = 25.5210(3) Å, b = 15.0899(13) Å, c = 19.9828(12) Å, β= 94.334(3)°, V = 7673.6(9) Å^3, Z = 4, T = 120 K, ρ_{calcd} = 1.740 Mg m^{-3}, μ(MoKα) = 2.305 mm^{-1}, 34057 reflections measured, 7337 unique (R_{int} = 0.0785) used in all calculations. The final wR_2 was 0.2724 (all data) and R_1 (5355 with I>2\s(I)) = 0.0815. Goodness-of-fit indicator 1.061. Maximum residual electron density 1.043 e Å^{-3}. CCDC 1829174 contains the crystallographic data.

Spectroscopic and Electrochemical Studies. The positive-ion mode matrix-assisted laser desorption/ionization time-of-flight (Bruker, German) was employed for the mass characterization. UV-vis-NIR spectrum of the purified Th@C_1(11)-C_{86} was measured in CS_2 solution with a Cary 5000 UV-vis-NIR spectrophotometer (Agilent, U.S.A). The Raman spectrum was obtained on a Horiba Lab RAM HR Evolution Raman spectrometer using a laser at 633 nm.

Electrochemical Studies. Cyclic voltammetry (CV) was obtained in o-dichlorobenzene using a CHI-660E instrument. A conventional three-electrode cell consisting of a platinum counter-electrode, a glassy carbon working electrode, and a silver reference electrode was used for the measurement. (n-Bu)$_4NPF_6$ (0.05 M) was used as the supporting electrolyte. The CV was measured at a scan rate of 100 mV/s.

Computational details

All the calculations were carried out using density functional theory (DFT) with the ADF 2017 package. [6] The BP86 functional and Slater triple-zeta polarization basis sets (BP86-DG3/TZP) were used, including Grimme dispersion corrections. [7] Frozen cores consisting of the 1s shell for C and the 1s to 5d shells for Th were described by means of single

Slater functions. Scalar relativistic corrections were included by means of the ZORA formalism. Frequency calculations of all optimised Th@C_1(11)-C_{86} geometries confirm that they correspond to minima. First oxidation and reduction potentials were computed at the same BP86-DG3/TZP level of theory, with dichlorobenzene as solvent by means of the COSMO model.

A data set collection of computational results is available in the ioChem-BD repository [8] and can be accessed via http://dx.doi.org/10.19061/iochem-bd-2-34.

References

1. W. Cai, L. Abella, J. Zhuang, X. Zhang, L. Feng, Y. Wang, R. Morales-Martinez, R. Esper, M. Boero, A. Metta-Magana, A. Rodriguez-Fortea, J. M. Poblet, L. Echegoyen and N. Chen, *J. Am. Chem. Soc.*, 2018, **140**, 18039-18050.
2. Z. Slanina, S.-L. Lee, F. Uhlík, L. Adamowicz and S. Nagase, *Theor. Chem. Acc.*, 2007, **117**, 315-322.
3. Z. Slanina and S. Nagase, *ChemPhysChem* 2005, **6**, 2060-2063.
4. Z. Slanina and L. Adamowicz, *Thermochim. Acta*, 1992, **205**, 299-306.
5. G. Sheldrick, *Acta Crystallographica Section A*, 2008, **64**, 112-122.
6. G. te Velde, F. M. Bickelhaupt, E. J. Baerends, C. Fonseca Guerra, S. J. A. van Gisbergen, J. G. Snijders and T. Ziegler, *J. Comput. Chem.*, 2001, **22**, 931-967.
7. S. Grimme, S. Ehrlich and L. Goerigk, *J. Comput. Chem.*, 2011, **32**, 1456-1465.
8. M. Álvarez-Moreno, C. de Graaf, N. López, F. Maseras, J. M. Poblet and C. Bo, *J.Chem. Inf. Mode.*, 2015, **55**, 95-103.